# Ethylene signaling increases reactive oxygen species accumulation to drive root hair initiation in *Arabidopsis thaliana*

R. Emily Martin[a], Eliana Marzol[c], Jose M. Estevez[b,c], Gloria K. Muday[a*]

[a] Departments of Biology and Biochemistry and the Center for Molecular Signaling, Wake Forest University, 1834 Wake Forest Road, Winston-Salem, NC 27109
[b] Fundación Instituto Leloir and IIBBA-CONICET. Av. Patricias Argentinas 435, Buenos Aires C1405BWE, Argentina.
[c] Centro de Biotecnología Vegetal, Facultad de Ciencias de la Vida, Universidad Andres Bello and ANID - Millennium Science Initiative Program - Millennium Institute for Integrative Biology (iBio), Santiago, Chile.

*Corresponding author, email**:** muday@wfu.edu

**Author Contributions:** REM conceived the research plan, designed and performed experiments and data analysis and wrote the article, EM and JME designed and prepared genetic constructs and provided editorial input into the writing, GKM conceived the research plan, supervised the project, and provided editorial input into the writing.

**Competing Interest Statement:** The authors declare no conflicts of interest.

**Classification:** Biological Sciences – Plant Biology

**Keywords:** Ethylene, reactive oxygen species, root hairs, peroxidase, RBOH

## ABSTRACT

Root hair initiation is a highly regulated aspect of root development. The plant hormone, ethylene, and its precursor, 1-amino-cyclopropane-1-carboxylic acid (ACC), induce formation and elongation of root hairs. We asked whether elevated ethylene induced root hair formation by increasing reactive oxygen species (ROS) synthesis in hair cells. Using confocal microscopy paired with redox biosensors and dyes, we demonstrated that treatments that elevate ethylene levels led to increased ROS accumulation in hair cells prior to root hair formation. In two ethylene-insensitive mutants, *etr1-3* and *ein3/eil1*, there was no increase in root hair number or ROS accumulation. Conversely, *etr1-7,* a constitutive ethylene signaling receptor mutant, has increased root hair formation and ROS accumulation similar to ethylene-treated wild type seedlings. The *rhd2-6* mutant, with a defect in the gene encoding a ROS synthesizing Respiratory Burst Oxidase Homolog C (RBOHC), showed impaired ethylene-dependent ROS synthesis and root hair formation and decreased RBOH enzyme activity compared to Col-0. To identify additional proteins that drive ROS induced root hair formation, we examined a time course root transcriptomic dataset examining Col-0 grown in the presence of ACC and identified *PRX44* and other positively regulated transcripts that encode class III peroxidases (PRXs). The *prx44-2* mutant has decreased root hair initiation and ROS accumulation when treated with ACC compared to Col-0 and *pPRX44*::GFP fluorescence is increased in response to ACC treatment. Together, these results support a model in which ethylene increases ROS accumulation through RBOHC and PRX44 to drive root hair formation.

56 **SIGNIFICANCE STATEMENT**

57 Root hairs are essential for water and nutrient acquisition and anchorage in soil. The hormone ethylene
58 increases both root hair initiation and elongation. Short-term treatment with ethylene and its precursor,
59 ACC, increased reactive oxygen species (ROS) accumulation in trichoblast cells prior to root hair initiation.
60 Ethylene signaling through the ETR1 receptor and transcription factors, EIN3/EIL1, increased ROS and
61 root hair initiation. Genetic and biochemical approaches identified ROS producing enzymes that are
62 regulated by ethylene signaling and required for root hair initiation. Ethylene signaling increased activity of
63 RBOHC and elevated transcript abundance of a class III peroxidase, PRX44, to drive root hair initiation.
64 Our findings demonstrate that ethylene-induced root hair initiation is dependent on changes in ROS
65 homeostasis.

66 **INTRODUCTION**

67 The initiation of root hairs is genetically programmed and environmentally sensitive, making them
68 an ideal model for studying single cell development in plants. Root hairs are single-cell extensions that
69 differentiate from longitudinal epidermal cell files, known as trichoblasts (1, 2). These structures rapidly
70 respond to environmental changes and act to increase root surface area to allow for efficient water and
71 nutrient uptake (3), while also anchoring plants in soil to reduce erosion (4). In Arabidopsis, the root
72 epidermis consists of an alternating pattern of trichoblasts, which form root hairs, and atrichoblasts, which
73 are non-hair forming cells (2, 5). Root hair formation is dictated by cell positioning; epidermal cells overlying
74 two cortical cells will become hair forming cells, while those overlying one cortical cell will become non-hair
75 cells (2, 6). Root hair development is separated into two processes: root hair initiation and root hair
76 elongation (7). Prior to initiation, RHO Of Plants (ROP) proteins accumulate at the future site of initiation
77 (8), this is followed by actin polymerization along which vesicles move to deposit membrane allowing for
78 polarized tip growth (2). During tip growth, tip focused reactive oxygen species (ROS) (9, 10) and $Ca^{2+}$
79 gradients (11) drive exocytosis of the cell wall and membrane materials driving subsequent root hair
80 elongation. These processes are separable as mutants with impaired root hair initiation or elongation have
81 been identified (12, 13)

82 Genetic screens in *Arabidopsis thaliana* have provided a wealth of insight into the proteins that
83 drive root hair development (14-16). For example, the mutants *transparent testa glabra (ttg)*, *glabra2 (gl2)*,
84 and *werewolf (wer)* have root hairs that form from both trichoblast and atrichoblast cells (16-18). Many of
85 the protein products of these mutants have been mapped to transcriptional cascades that drive root hair
86 differentiation (19). In non-hair cells, a transcriptional complex comprised of three transcription factors
87 (TFs), WER, GLABRA 3 (GL3), or its functionally redundant ENHANCER OF GLABRA (EGL3), and TTG1,
88 function as a transcriptional activator of the GL2 protein, which leads to repression of root hair initiation (2,
89 20). In trichoblasts, *WER* expression is repressed, which allows for the formation of an alternate
90 transcriptional complex comprised of CAPRICE (CPC) or the functionally redundant proteins ENHANCER
91 OF TRY AND CPC1 (ETC1), ETC3, or TRYPTICHON (TRY) (21). When this pathway is active, GL2 is not
92 expressed and root hair initiation proceeds (2).

93 Another genetic screen identified the *root hair defective* (*rhd*) mutants which have impaired root
94 hair initiation, elongation or structure (12, 13). In one of these mutants, *rhd2,* the mutation was mapped to
95 the *RBOHC* (respiratory burst oxidase homolog C/NADPH oxidase) gene (9). The *rhd2* mutant was
96 identified for altered root hair elongation (12), but was recently reported to also have impaired root hair
97 formation (10). RBOHs are integral plasma membrane proteins that produce superoxide, which can be
98 dismutated to hydrogen peroxide via superoxide dismutase (SOD) or other non-enzymatic mechanisms
99 (22). $H_2O_2$ can then enter into the cell through aquaporins (23), where it can act as a signaling molecule to
100 drive cellular processes. Signaling induced ROS regulates protein function by reversibly oxidizing cysteine
101 residues to sulfenic acids (Cys-SOH) (24).

102 There are 10 RBOH family members (RBOHA-RBOHJ) in Arabidopsis and each play distinct roles
103 in organ development and stress response (22). RBOHs can be regulated transcriptionally or enzymatically
104 by a number of mechanisms, including calcium binding, phosphorylation, and phosphatidic acid binding
105 (25-27). RBOH-induced ROS production is also regulated by hormone signaling, as many plant hormones
106 generate ROS as a mechanism to drive growth and developmental processes (22, 27-29). For example,
107 abscisic acid (ABA), a hormone involved in abiotic stress response, has been shown to induce RBOH-
108 derived ROS production to prevent water loss in leaves (29). Auxin induces root hair elongation through a
109 localized increase in ROS (30), suggesting that RBOH may drive hormone induced root hair formation.

110 The plant hormone ethylene enhances root hair initiation and elongation. Treatment with ethylene,
111 or its precursor 1-amino-cyclopropane-1-carboxylic acid (ACC), leads to proliferation of root hairs, with
112 substantial increases in length (31). The ethylene induction of root hairs occurs through the canonical
113 ethylene signaling pathway, which is initiated when ethylene binds to one of the five receptors, ETR1,
114 ERS1, ETR2, ERS2, or EIN4 (32, 33). When ethylene is absent, the receptors are in the “on state” leading
115 to activation of the CTR1 Raf-like kinase (34); this turns the pathway off via phosphorylation and subsequent
116 degradation of the EIN2 transmembrane protein (35, 36). When ethylene binds to its receptors they shift to
117 the “off state” which prevents activation of CTR1. This allows for cleavage and translocation of the EIN2 C-
118 terminus into the nucleus (36, 37) where it stabilizes the EIN3/EIL1 TFs leading to ethylene responsive
119 gene expression. Previous work has shown that ethylene regulates root hair elongation through the EIN3

120 transcription factor (38). EIN3 physically interacts with RHD6, a known positive regulator of root hair
121 development, to form a transcriptional complex that binds to and induces expression *RSL4*. This
122 transcriptional regulation results in increased root hair length (38). However, the mechanistic events that
123 drive ethylene-induced root hair initiation have not been fully described, and the role of ROS as a
124 downstream molecule in ethylene-induced root hair development has not been reported.

125 We asked whether ethylene acts to increase ROS levels to drive root hair initiation. Using
126 fluorescent dyes and biosensors that report ROS levels, we examined ROS accumulation after ACC
127 treatment in trichoblast cells in the differentiation zone. We asked whether this response is dependent on
128 ETR1 receptor activity and EIN3 TF activity. We also examined the role of RBOHC and class III peroxidase
129 enzymes in ethylene-dependent ROS synthesis. Together these experiments demonstrated that ROS is a
130 signaling molecule in ethylene induced root hair development and identified several enzymes that
131 participate in producing ethylene-induced ROS.

132 **RESULTS**

133 **Root hair number was increased in ACC treated roots**

134 To understand the role of ethylene signaling in root hair initiation we examined the effects of short-
135 term treatments with the ethylene precursor, ACC, on the number and position of root hairs in 5 day old
136 seedlings. Root hairs were visualized in wild type (Col-0) seedlings grown in the presence of 1 μM ACC
137 for 4 hours (Figure 1A). The root tip was divided into three 500 μm zones starting from the root tip and he
138 number of root hairs formed in each zone was quantified Figure 1B). In zone 1, root hairs did not form in
139 either untreated or ACC-treated seedlings. In zone 2, there were very few root hairs in untreated roots,
140 however, ACC-treatment increased the number of root hairs by 10-fold. There was also a 2-fold increase
141 in root hair number in zone 3 of ACC-treated seedlings compared to untreated controls. These data suggest
142 that ACC-induced root hair initiation begins between 500 and 1000 μM from the root tip. Therefore, to
143 understand the mechanisms driving the process of root hair initiation our experiments focused on this
144 region.

145 ACC treatment also resulted in a shorter primary root due to reduced elongation of root cells (39),
146 therefore we asked whether the increase in root hairs seen with ACC treatment was due to shorter cell
147 length resulting in more root hairs in zone 2. To explore this possibility, roots treated with or without ACC
148 for 4 hours were stained with the cell wall specific dye, propidium iodide (PI). We then measured the length
149 of 5 epidermal cells from 6-8 roots per treatment condition, measuring the length of cells at either end and
150 in the middle of zone 2 (Figure S1). We found that there was no difference in cell length after 4 hours of
151 ACC treatment compared to untreated controls at both ends of this zone. These results are consistent with
152 short term and low dose ACC treatments increasing root hair number by inducing more root hair forming
153 trichoblasts in zone 2, rather than as an indirect effect of a shorter primary root.

154 **ROS accumulation was increased in ACC treated roots**

155 We asked whether ethylene leads to elevated reactive oxygen species (ROS) to drive ethylene-
156 induced root hair initiation. We examined ROS dependent gene expression along the root using the
157 ZAT12p-ROS ratiometric biosensor (40). This reporter construct contains the promoter of the ROS sensitive

158 transcription factor, ZAT12, driving GFP and the constitutive ubiquitin10 promoter driving mCherry. We
159 compared the fluorescent signal of ZAT12p-ROS in the presence and absence of ACC as visualized by
160 laser scanning confocal microscopy (LSCM), with GFP reported as green and mCherry reported as
161 magenta (Figure 1C). The ratio of signal of GFP to mCherry was quantified across the entire root as a
162 distance from the root tip. In ACC-treated roots, the GFP/mCherry ratio increased beginning at
163 approximately 500 μm from the root tip, which corresponded to zone 2, where root hair induction was
164 maximal upon treatment with ACC (Figure 1D).

165 We also used the hydrogen peroxide selective dye, Peroxy-Orange 1 (PO1) to ask whether there
166 were cell type-specific increases in ROS in response to ACC. PO1 is a permeable, boronate-based dye
167 that is non-fluorescent in its reduced form, but becomes fluorescent when irreversibly oxidized by $H_2O_2$
168 (41). In Col-0 roots, PO1 fluorescence was visualized using LSCM in zone 2 of roots treated with and
169 without ACC for 4 hours (Figure 1E). In Arabidopsis, root hairs form in alternating patterns, so that every
170 root hair forming cell (trichoblast) is adjacent to a non-hair cell (atrichoblast). We quantified ROS
171 accumulation by analyzing PO1 signal after confocal imaging, by drawing a line across the width of the root
172 that spans 5 epidermal cell files so that the PO1 signal in 3 trichoblasts and 2 atrichoblasts was quantified
173 (Figure 1F). We found that PO1 accumulation in trichoblasts of untreated seedlings was slightly, but not
174 significantly higher than atrichoblasts. In trichoblast cells in ACC treated seedlings, there was a significant
175 increase in PO1 accumulation in ACC-treated trichoblasts as compared to trichoblasts of untreated
176 seedlings and compared to atrichoblasts of both untreated and ACC treated seedlings. In contrast, there
177 were no changes in PO1 in the atrichoblasts suggesting that ACC treatment increased ROS levels in only
178 the cells that formed root hairs (Figure 1F).

179 **ROS accumulation increased prior to root hair emergence**

180 To determine whether ethylene-induced ROS accumulation drives root hair emergence, we asked
181 whether the ACC-induced ROS increases were detectable prior to the first ACC-induced root hair initiation.
182 Wild type Col-0 seedlings were treated with ACC for either 2 or 4 hours and PO1 fluorescence was
183 visualized in trichoblasts that did not have a root hair bulge (Figure 2A). These trichoblasts were chosen
184 for quantification to determine whether ACC-induced ROS increases were seen in hair forming cells prior

185 to root hair emergence. Total PO1 accumulation was measured in 5 individual trichoblasts per root treated
186 with and without ACC. Signal was quantified across the area of the entire cell and the average PO1 intensity
187 of 24-30 individual cells was reported (Figure 2B). Atrichoblast signal was not quantified as ROS levels did
188 not change in those cells (Figure 1F). Cells treated with ACC for 4 hours were not quantified because nearly
189 all of the trichoblasts in Zone 2 at this time point had already begun the process of root hair initiation (Figure
190 2C). These data showed a 1.3-fold increase in PO1 accumulation in hair cells of seedlings treated with
191 ACC for 2h as compared to untreated controls, when trichoblast cells that had not yet begun to initiate root
192 hairs were examined. These data are consistent with the hypothesis that ROS acts as a driver of root hair
193 initiation downstream of ethylene signaling.

194 **Ethylene signaling mutants showed altered ROS accumulation patterns and root hair phenotypes**

195 We examined ROS accumulation in response to ACC treatment in seedlings with mutations in
196 genes encoding key ethylene signaling proteins to ask whether this response was dependent on the
197 ethylene signaling pathway and downstream transcriptional responses. The number of root hairs and
198 average length were previously reported in loss-of-function and gain-of-function ethylene receptor mutants,
199 *etr1-7 and etr1-3,* and the transcription factor mutant *ein3eil1* in the presence and absence of ACC
200 treatment (39). *etr1-7* is a LOF mutant in which the ETR1 receptor is inactive, therefore the ethylene
201 signaling pathway is constitutively signaling and there are increased numbers of root hairs independent of
202 ACC addition, while *etr1-3* is a GOF mutant in which the ETR1 receptor is always active leading to an
203 inactive signaling pathway (39, 42). The double mutant *ein3eil1* has mutations in genes encoding EIN3 and
204 EIL1 TFs (43, 44). Both *etr1-3* and *ein3eil1* have reduced root hair initiation in response to ACC treatment
205 (39). We examined the PO1 distribution patterns in root hair cells with and without ACC treatment in these
206 three mutants. We visualized PO1 fluorescence via LSCM and saw that the constitutive ethylene signaling
207 mutant *etr1-7* had increased $H_2O_2$ in root hair cells and increased root hair initiation from these cells
208 regardless of ACC treatment (Figure 3). The opposite response was seen in the ethylene-insensitive *etr1-*
209 *3* and *ein3eil1* mutants, as they showed reduced PO1 signal and root hair initiation and no increase in $H_2O_2$
210 accumulation in the presence of ACC. Together, these results suggest that the ETR1 receptor and
211 EIN3/EIL1 TFs are required for ethylene-induced ROS accumulation and root hair initiation.

212 To determine if the changes in ROS accumulation seen in response to ACC were due to ACC's
213 conversion to ethylene, we treated Col-0 seedlings with 0.05 ppm of ethylene gas for 4 hours followed by
214 PO1 staining and signal quantification as described above. We observed the same ROS accumulation
215 patterns in both treatment conditions, with PO1 fluorescence intensity values in trichoblasts of ethylene-
216 treated seedlings showing the same magnitude increase as root treated with ACC (Figure S2). This is
217 consistent with our results showing that ACC has no effect on root hair number or ROS accumulation in the
218 constitutive ethylene insensitive signaling mutants, *etr1-3* and *ein3/eil1* and in the constitutive ethylene
219 signaling receptor mutant, *etr1-7,* in the absence (or presence) of ACC

220 **The RBOHC knockout mutant, *rhd2-6*, showed decreased ROS accumulation after ACC treatment**

221 It has been previously reported that the respiratory burst oxidase homolog C (RBOHC) is involved
222 in ROS production and subsequent root hair elongation (9). We have also shown that there is decreased
223 ROS in root hairs of the *rhd2-6* mutant, which has an insertion mutation in the *RBOHC* gene (10). Therefore,
224 we examined root hair numbers via light microscopy and PO1 accumulation patterns via LSCM in ACC-
225 treated *rhd2-6* (*rbohc*) seedlings (Figure 4). Root hair number and root hair length in the ACC-treated *rhd2-*
226 *6* mutant was significantly less than ACC-treated Col-0, suggesting that RBOHC contributes to both
227 ethylene-induced root hair initiation and elongation (Figure 4B). We found that, in the ACC-treated *rhd2-6*
228 mutant, the significant increase in $H_2O_2$ fluorescence accumulation seen in Col-0 hair cells was at lower
229 levels in the mutant (Figure 4C-D), suggesting that RBOHC contributes to ethylene-induced ROS
230 accumulation. To determine if other RBOHs that are expressed in root tissue contributed to ethylene-
231 induced ROS accumulation, PO1 accumulation patterns were examined in the *rbohd/f* double mutant. No
232 change was seen in ROS levels in hair cells of *rbohd/f*, suggesting that these RBOHs do not contribute to
233 ethylene-induced ROS synthesis in root hair cells (Figure S3).

234 **RBOH enzyme activity was increased in response to ethylene signaling**

235 Elevated ethylene may either increase *RBOHC* transcript abundance or enzyme activity. We
236 examined several transcriptomic datasets with ACC or ethylene treated roots and found a subtle change in
237 the *RBOHC* transcripts, but not significant enough to pass the filtering on this transcriptomic analysis (39,
238 45) (Table S1). To determine if ethylene signaling regulated RBOH enzyme activity, a spectrophotometric

239 assay using nitro blue tetrazolium (NBT) dye as an electron acceptor, was performed. NBT is reduced by
240 superoxide to monoformazan and this reduction can be detected at 530 nm. This experiment was performed
241 in protein extracts from 7-day old roots of Col-0 and *rhd2-6* treated with and without ACC for 4 hours. Older
242 roots were used in this experiment to obtain an adequate amount of protein for these assays. There was a
243 significant 2-fold increase in monoformazan production in protein extracts of Col-0 roots treated with ACC
244 for 4 hours compared to controls (Figure 4E). The enzyme activity of roots of untreated *rbohc/rhd2-6* was
245 3-fold lower than roots of untreated Col-0 and the enzyme activity in the presence of ACC was significantly
246 reduced relative to ACC treated Col-0 (Figure 4E). These data are consistent with previous results
247 indicating that the RBOHC enzyme constitutes the majority of the superoxide production in roots (10, 22).

248 **Transcription of *PRX44* increases with ACC treatment driving ROS accumulation and ethylene-**
249 **induced root hair initiation**

250 The *ein3/eil1* transcription factor mutant has reduced root hair initiation and a reduction in PO1
251 signal in trichoblasts suggesting that there is transcriptional regulation of ROS producing enzymes that
252 drive root hair initiation. We examined a previously published microarray time course experiment in roots
253 treated with ACC (39) to identify candidate transcriptional targets profiling the expression pattern of
254 transcripts encoding both ROS producing enzymes and proteins linked to trichoblast cell specification.
255 ROP2, ROPGEF3, ROPGEF4, GL2, RSL4 and RHD6, which are linked to root hair initiation, showed no
256 transcriptional response to ACC treatment and primers that recognize RSL1 and RSL2 are not present on
257 the microarray and could not be examined in this dataset (Table S1). A number of transcripts encoding
258 class III PRXs changed in abundance in response to ACC, including the transcript encoding *PRX44,* which
259 increased by 3-fold. Class III peroxidases are specific to plants and exist in large multigene families. They
260 have been implicated in root hair tip growth, as null mutants have shorter root hairs compared to wild type
261 (30). Recent work has shown that auxin induces expression of genes encoding four class III peroxidases
262 (PRX), which results in an increase in both root hair length and ROS accumulation (30), however, the role
263 of ethylene signaling in regulating class III PRX expression to modulate root hair initiation or elongation has
264 not been reported.

265 We examined control and ACC-treated seedlings harboring the *PRX44* promoter driving GFP and
266 examined GFP expression via LSCM. Seedlings treated with ACC showed a statisictally significant >2-fold
267 increase in GFP fluorescence, suggesting that the *PRX44* promoter is induced downstream of ethylene
268 signaling (Figure 5A-B). We also asked whether these peroxidases participate in ACC-regulated root hair
269 initiaion. We examined root hair numbers via light microscopy in Col-0 and *prx44-2* seedlings treated with
270 and without ACC. There were significantly fewer root hairs in *prx44-2* controls compared to Col-0 controls
271 and the effect of ACC on root hair initiation was reduced in the *prx44-2* mutant, although there was still a
272 significant response to ACC (Figure 5C-D). The root hairs in the ACC-treated mutant also appeared shorter
273 compared to Col-0, which is consistent with the phenotype that has been reported in response to auxin
274 treatment (30). When PO1 accumulation patterns were examined via LSCM, we observed no significant
275 increase in PO1 accumulation in hair cells of *prx44-2* seedlings treated with ACC (Figure E-F). We also
276 examined *prx73-4*, since the transcripts encoding PRX73 has also been reported to be induced with auxin
277 treatment to drive root hair elongation (30) and these transcripts profound increases in response to ACC
278 treatment (Table S1). The *prx73-4* mutant showed no change in PO1 fluorescence in the presence or
279 absence of ACC as compared to Col-0 (Figure S4) and showed no changes in root hair initiation after ACC
280 treatment. These combined data indicate that the class III PRX44 is transcriptionally regulated by ethylene
281 and contributes to ethylene induced ROS accumulation and root hair initiation.

282 **DISCUSSION**

283 Ethylene is a key hormonal regulator of root hair initiation and elongation (34, 46). Although the
284 proteins that drive ethylene signaling are well characterized, the downstream proteins that control the root
285 hair developmental processes have received less study. Reactive oxygen species (ROS) are critical for
286 both root hair initiation and elongation (9, 10, 47, 48). In root hairs, one source of ROS is the NADPH
287 oxidase (NOX)/respiratory burst oxidase homolog C (RBOHC) that is localized to root hairs to facilitate cell
288 wall loosening and subsequent tip focused $Ca^{2+}$ accumulation leading to cell elongation (9). The plant
289 hormone auxin also induces ROS to drive root hair elongation (30), so we asked if ROS is a signaling
290 molecule in ethylene-induced root hair development. In this study, we examined the effects of ethylene
291 signaling on root hair initiation and ROS accumulation to determine if increased ethylene drives root hair
292 initiation through regulation of ROS producing enzymes and subsequent ROS accumulation in trichoblasts
293 from which root hairs form.

294 We asked whether ethylene signaling induced root hair initiation at the root tip by examining root
295 hair number of Col-0 and ethylene signaling mutant seedlings grown in the presence of low concentrations
296 of the ethylene precursor, ACC (1 μM), for 4 hours. There was a significant increase in the number of
297 trichoblasts that formed root hairs in ACC treated seedlings compared to untreated controls. This root hair
298 induction was most pronounced in a region starting 500 μm from the root tip and ending at 1000 μm, which
299 we refer to as zone 2. Consistent with this effect occurring through ACC conversion to ethylene, the ACC
300 induction in root initiation is lost in ethylene insensitive mutants *etr1-3* and *ein3eil1*, consistent with our prior
301 reports (39) other prior studies which showed that ACC-inhibited root elongation, gravitropism, and lateral
302 root formation are lost in the ethylene insensitive *ein2-5* and *etr1-3* mutants at this dose of ACC under our
303 growth conditions (39, 49, 50). These findings are also consistent with efficient conversion of ACC to
304 ethylene and ACC effects on ROS synthesis and root hair initiation due to ethylene signaling responses.

305 We asked whether ACC treatment increased ROS levels in wild-type seedlings using both genetic
306 and chemical ROS probes. Using a ratiometric reporter of ROS-induced gene expression, ZAT12p-ROS,
307 we found that in ACC-treated roots, ROS dependent gene expression was increased in a region spanning
308 from 200 to 1000 μm from the root tip. Expression was quantified in the entire root and elevated

309 fluorescence was seen in a region 500-1000 μm from the root tip (zone 2) in ACC treated roots compared
310 to untreated controls. We also used a boronate based hydrogen peroxide sensor, PO1, and found that $H_2O_2$
311 accumulation was elevated in the trichoblast cells in zone 2 and significantly increased within 2 hours after
312 ACC treatment, prior to the initiation of root hair bulges. We also performed treatments with 0.05 ppm of
313 ethylene gas and demonstrated that ethylene gas also increases PO1 signal in trichoblasts prior to root hair
314 initiation. These data suggest that ROS act downstream of ethylene signaling in zone 2 of the root, and that
315 these signals occur prior to root hair initiation.

316 We next asked which components of the ethylene signaling pathway were required for ethylene-
317 induced ROS synthesis in trichoblasts of zone 2. ROS accumulation was monitored in two *etr1* mutants: a
318 constitutive ethylene signaling *etr1-7* allele and an ethylene insensitive *etr1-3*, as well as the TF null mutant
319 *ein3eil1.* Compared to Col-0, *etr1-7* exhibited an increase in ROS accumulation and root hair number in the
320 presence and absence of ACC treatment, while these responses were lost in the ACC-treated ethylene
321 insensitive *etr1-3* and *ein3eil1* mutants. These results are consistent with the ethylene receptor ETR1 and
322 the EIN3/EIL1 master transcriptional regulators being required for ethylene-induced ROS accumulation and
323 root hair initiation.

324 To determine if RBOH/NOXs were contributing to ethylene-induced ROS synthesis, we asked
325 whether the RBOHC enzyme was required to drive ROS accumulation and root hair initiation. Based on
326 previous work detailing the role of RBOHC in root hair initiation and growth (9, 10), we asked whether this
327 enzyme was contributing to ethylene-induced ROS accumulation and subsequent root hair initiation and/or
328 elongation. ACC treated *rhd2-6*, which is an *RBOHC* null mutant, had reduced ROS accumulation in
329 trichoblasts compared to Col-0 and ACC failed to increase the number of initiated root hairs. The abundance
330 of RBOHC transcripts showed small changes in response to ACC treatment (39), while there was more
331 than a 2-fold increase in RBOH activity in response to ACC treatment and there was a 3-fold reduction in
332 activity in the *rhd2-6* (*rbohc*) mutant. These data suggest that ethylene signaling induces superoxide
333 production in roots via increases in RBOHC enzyme activity to drive root hair initiation and elongation.
334 However, since there is still some ACC induction of root hair initiation in the *rhd2-6* mutant, these data
335 suggest that initiation may require additional proteins.

336 We examined previously published ACC and ethylene transcriptomic datasets to search for
337 transcripts encoding root hair specification proteins and ROS producing enzymes that are ethylene
338 regulated. Although ACC did not change abundance of transcripts encoding ROP2, ROPGEF3, ROPGEF4,
339 GL2, RHD6, or RSL4, we identified several transcripts encoding class III peroxidase enzymes that showed
340 substantial increase in response to ACC. *PRX44 and PRX73*, showed a significant increase in abundance
341 after 4 hours of ACC treatment. We then examined the effects of ACC treatment on the null mutant *prx73-*
342 *4* and *prx44-2* and found decreased ROS accumulation in root hair forming trichoblasts in *prx44-2* and no
343 effect in *prx73-4* compared to Col-0. The decreased PO1 signal in *prx44-2* was accompanied by significant
344 reductions in the number of root hairs formed in this same root region. We examined a PRX44 promoter
345 driven GFP fusion protein (*pPRX44*::GFP) observing its expression in trichoblast cells in zone 2 and
346 demonstrated that ACC treatment leads to significant increases in fluorescence intensity compared to
347 untreated controls. Together these experiments implicate Class III peroxidase enzymes in root hair
348 initiation.

349 These peroxidase enzymes have also been implicated in regulation of root hair elongation, as null
350 mutants treated with auxin have shorter root hairs and less ROS compared to wild type (30). Class III
351 peroxidases are specific to plants and exist in large multigene families. Reverse genetic studies have shown
352 that they are involved in lignification, cell elongation, stress defense and seed germination (51). At least 73
353 Arabidopsis genes encode class III peroxidases, however, due to their redundancy and lack of information
354 on their substrate specificity, their functions and mechanisms of regulation are relatively unclear. They are
355 secreted into the cell wall or surrounding medium and are involved in a number of different reactions that
356 involve both ROS consumption and production (52, 53). However, previous work regarding peroxidase
357 activity in root hair elongation suggests that they act as ROS producers, as 3 PRXs have been reported to
358 be involved in increasing the ROS gradient required for root hair elongation (30)

359 To summarize our findings on ethylene-dependent root hair initiation via increased ROS synthesis
360 and to tie these findings with other studies, we present a model in Figure 6. ACC treatment induces
361 ethylene signaling, which acts through the ETR1 receptor and the canonical signaling pathway which then
362 increases the activity of EIN3/EIL1 TFs. EIN3/EIL1 binds to the root hair specific TF RHD6 to induce RSL4

363 expression and root hair elongation (38). Root hair growth is controlled by several proteins that eventually
364 activate the RHD6 TF. Downstream of RHD6, the RSL4 TF is activated and it defines final root hair length
365 based on its level of expression (30, 54). Previous work has shown that EIN3 physically interacts with RHD6
366 to form a transcriptional complex that coactivate RSL4 to promote root hair elongation (38). However, in
367 our microarray dataset (39), *RSL4* transcript abundance only showed slight changes in response to ACC
368 treatment (Table S1). It has also been shown that auxin treatment results in increased RSL4 transcript
369 abundance, which binds to the promoters of RBOH and four class III peroxidase (*PRX*) genes, including
370 *PRX44*, to drive ROS synthesis in root hair cells. RSL4 activation via auxin induces class III peroxidase and
371 *RBOH* expression, which leads to ROS accumulation required to drive root hair elongation (30). We find
372 that ACC treatment increases activity of RBOHC enzymes leading to increased ROS and root hair
373 elongation, without changing the abundance of *RBOHC* transcripts. Additionally, ACC treatment leads to
374 the transcriptional regulation of class III peroxidases (39), resulting in ROS production and root hair
375 initiation. Further investigation regarding the mechanisms of ethylene-regulated ROS synthesis is required.
376 For example, one important question to be answered is how ethylene signaling regulates RBOH activity.
377 This could occur through a number of different mechanisms, such as calcium binding or phosphorylation,
378 which are known to regulate RBOH enzymes (27). It is also unknown as to whether ethylene regulates
379 class III peroxidase expression via EIN3 or an alternate transcriptional mechanism, or if ethylene also
380 regulates class III peroxidase enzyme activity.

381

382 **MATERIALS AND METHODS**

383 **Growth conditions and root hair quantification**

384 All Arabidopsis mutants were in the Col-0 background. The *etr1-7*, *etr1-3* (AT1G66340), *ein3-1*
385 (AT3G20770) *eil1-1* (AT2G27050) double and *rhd2-6* (AT5G51060) mutants have all been described
386 previously (10, 39, 42, 55). The ZAT12p-ROS construct was generously provided by Won-Gyu Choi (40).
387 *prx44-2* (AT4G06010) and *prx73-4* (AT5G67400) were obtained from the Arabidopsis SALK center
388 (SALK_057222C and SALK_020724, respectively), the mutations were verified by PCR, and homozygous
389 lines were isolated. The transcriptional reporter *pPRX44*::GFP transgenic line was described previously
390 (56). Seeds were sterilized in 70% ethanol for approximately 5 minutes and grown on 100 x 15 mm Petri
391 dishes containing 25 mL media. Seedlings were grown on 1x MS supplemented with 1% sucrose, vitamins
392 (1 µg/ml thiamine, 0.5 µg/ml pyridoxine and 0.5 µg/ml nicotinic acid), 0.05% MES (w/v) and 0.8% (w/v)
393 agar. Media pH was 5.5. Micropore tape was used to seal the top of the Petri dish and plated seeds were
394 stratified at 4◦ C in darkness for 2 days. Plants were grown under 24h light from T5 fluorescent lights at
395 120-150 µmol photons $m^{-2}$ $s^{-1}$. Seedlings were grown for 5 days on control media and then transferred to
396 media containing 1 µM ACC and grown for 4 hours or other indicated times. To examine root hairs, 5-day
397 old seedlings were imaged using bright-field on an Axio Zoom V16 stereomicroscope. Extended depth of
398 focus was used to combine z-stack images. Root hairs were quantified using Fiji/ImageJ software in three
399 zones (0-500 µm, 500-1000 µm, 1000-1500 µm) starting from the root tip.

400 **Confocal imaging of dyes and reporters of ROS levels**

401 $H_2O_2$ was visualized with Peroxy-Orange 1 (PO1). PO1 was dissolved in DMSO to make a 500 µM
402 stock and was further diluted in $H_2O$ to make a 50 µM working solution. Seedlings were incubated in PO1
403 for 15 minutes in the dark and were then rinsed with $H_2O$ and mounted in $H_2O$ for imaging. All seedlings
404 were imaged on a Zeiss 880 laser scanning confocal microscope using a 10x objective. PO1 was excited
405 with a 488 nm laser at 0.25% power and emission was collected between 544-695 nm. Images were
406 analyzed using Fiji/ImageJ software. Plot profiles were taken across the epidermal cell files of maximum
407 intensity projections using a 20-pixel line and values were averaged within each cell file.

408 5-day old seedlings harboring the ZAT12p-ROS construct were mounted in $H_2O$ and excited with
409 488 and 561 nm lasers at 6% and 1.2% laser power, respectively. GFP emission was collected at 521 nm
410 and mCherry emission was collected at 593 nm. Fiji/ImageJ software was used to generate two single
411 channel images to form individual GFP and mCherry channels. Plot profiles were taken using a 250-pixel
412 wide line to measure fluorescence of the entire root. Measurements were taken starting at 200 µm back
413 from the root tip and ending at 1500 µm. Ratios were generated by dividing the GFP channel by mCherry
414 using the Image Calculator tool (Process/Image Calculator).

415 **PI staining and *proPRX44*::GFP imaging**

416 Cell walls were stained with 0.5 µg/mL propidium iodide (PI) dissolved in $H_2O$. 5 day old seedlings
417 treated with and without ACC were incubated in PI for 4 minutes before imaging. Fluorescence was
418 visualized using a 561 nm laser at 0.15% and emission spectra set to 561-695 nm. These settings were
419 used for all images. Optical slices of the top section of the root to show epidermal cells and maximum
420 intensity projections of z-stack images are shown in Figure S1. Fiji software was used to measure cell
421 length of 3 epidermal cells per root using optical slices of the top section of the root. Cells were chosen at
422 the bottom of zone 2 (cell 1, in the middle (cell 2), and at the top (cell 3). 4 cells of each of the 3 cell types
423 were averaged and are shown in FS1. 6-8 roots of both control and ACC treated seedlings. Transgenic
424 seeds harboring *pPRX44*::GFP were obtained from the lab of Dr. Jose Estevez, 5-day old seedlings were
425 mounted in $H_2O$ and excited with a 488 nm laser at 5% and emission was collected between 490-606 nm.
426 Seedlings were then stained with PI.

427 **DNA extraction and PCR for mutant genotype analysis**

428 T-DNA insertion lines were grown for approximately 2 weeks on media described above, then
429 transferred to soil and grown under 24h light at 50-80 µmol photons $m^{-2}$ $s^{-1}$. Leaves were harvested from 6
430 week old plants and stored in eppendorf tubes at -20° C prior to DNA extraction. Frozen leaves were ground
431 in DNA extraction buffer (100 mM Tris-HCl pH 8.0, 10 mM Na2EDTA, 100 mM $LiCl_2$, 1% (w/v) SDS).
432 Samples were then washed once with isopropanol and three times with 80% (v/v) ethanol. Finally, DNA
433 pellets were dried, resuspended in sterile $H_2O$ and stored at -20° C. Each PCR reaction contained 1X GoTaq
434 Polymerase, 1 µM of each primer, 1 uL of DNA and 5 µL $H_2O$. To confirm that mutants were homozygous

435 for the desired T-DNA insertion, one reaction was performed with primers (left primer and right primer)
436 flanking the left and right sides of in-tact genes while one reaction was performed with the right primer and
437 LBb1.3, which is a primer specific for the left border of the T-DNA insertion. PCR products were run on 0.8
438 % (w/v) agarose gels containing 0.002% SERVA DNA stain G.

439 **NADPH oxidase/RBOH enzyme assays**

440 Protein extract was isolated from seedlings grown on a nylon filter as described previously (39).
441 After 2 days of stratification and 7 days of growth under conditions described above, the nylon was
442 transferred to growth medium with and without 1 μM ACC for 4 hours. Roots were then cut from seedlings
443 and flash frozen in liquid nitrogen. Frozen samples were ground in liquid nitrogen using a mortar and pestle.
444 RBOH extraction buffer (50 mM Tris-HCl pH 7.5, 0.1 mM EDTA, 0.1% (v/v) Triton X-100, 1 mM $MgCl_2$, 10%
445 (v/v) glycerol) was then added to a plant material/buffer ratio of 1:3 (w/v). Samples were centrifuged and
446 supernatant was collected and desalted and concentrated using the Amicon Ultra-0.5 Centrifugal Filter
447 devices. RBOH reaction mixture (50 mM Tris-HCl pH 7.5, 1 mM $CaCl_2$, 0.1 mM nitroblue tetrazolium (NBT),
448 0.1 mM NADPH) was then mixed with protein extract at a 1:1 ratio. The reduction of NBT to monoformazan
449 was monitored spectrophotometrically at 530 nm. Monoformazan concentrations were calculated using a
450 12.8 $mM^{-1}cm^{-1}$ extinction coefficient. This assay was adapted in sweet peppers and has previously been
451 described (57).

452 **ACKNOWLEDGMENTS**

453 We would like to thank Dr. Brad Binder (University of Tennessee) and all Muday lab members for their
454 editorial input, and Dr. Glen Marrs and Dr. Heather Brown-Harding (Wake Forest University) for their help
455 with microscopy. This project was supported by the National Science Foundation (MCB-1716279 to GKM)
456 and a USDA Predoctoral Fellowship (NIFA 2021-67034-35113 to REM). Dr. Jose Estevez and Dr. Eliana
457 Marzol are investigators of the National Research Council (CONICET) from Argentina. Their work on this
458 project was supported by grants from ANPCyT (PICT2019-0015 to J.M.E. and PICT2018-0577 to E.M.). In
459 addition, this research was also funded by ANID – Programa Iniciativa Científica Milenio ICN17_022 and
460 Fondo Nacional de Desarrollo Científico y Tecnológico [1200010] to J.M.E.

461 **REFERENCES**


462 1. Leavitt R (1904) Trichomes of the root of vascular cryptograms and angiosperms. *Proceedings of*
463 *the Boston Society of Natural History* 31:273-313.
464 2. Salazar-Henao JE, Velez-Bermudez IC, & Schmidt W (2016) The regulation and plasticity of root
465 hair patterning and morphogenesis. *Development* 143(11):1848-1858.
466 3. Bruex A*, et al.* (2012) A Gene Regulatory Network for Root Epidermis Cell Differentiation in
467 Arabidopsis. *Plos Genet* 8(1).
468 4. De Baets S*, et al.* (2020) Micro-scale interactions between Arabidopsis root hairs and soil particles
469 influence soil erosion. *Commun Biol* 3(1).
470 5. Pemberton LMS, Tsai SL, Lovell PH, & Harris PJ (2001) Epidermal patterning in seedling roots of
471 eudicotyledons. *Ann Bot-London* 87(5):649-654.
472 6. Berger F, Haseloff J, Schiefelbein J, & Dolan L (1998) Positional information in root epidermis is
473 defined during embryogenesis and acts in domains with strict boundaries. *Curr Biol* 8(8):421-430.
474 7. Dolan L*, et al.* (1994) Clonal Relationships and Cell Patterning in the Root Epidermis of Arabidopsis.
475 *Development* 120(9):2465-2474.
476 8. Molendijk AJ*, et al.* (2001) Arabidopsis thaliana Rop GTPases are localized to tips of root hairs and
477 control polar growth. *Embo J* 20(11):2779-2788.
478 9. Foreman J*, et al.* (2003) Reactive oxygen species produced by NADPH oxidase regulate plant cell
479 growth. *Nature* 422(6930):442-446.
480 10. Gayomba SR & Muday GK (2020) Flavonols regulate root hair development by modulating
481 accumulation of reactive oxygen species in the root epidermis. *Development* 147(8).
482 11. Carroll AD*, et al.* (1998) Ca2+, annexins, and GTP modulate exocytosis from maize root cap
483 protoplasts. *Plant Cell* 10(8):1267-1276.
484 12. Schiefelbein JW & Somerville C (1990) Genetic-Control of Root Hair Development in Arabidopsis-
485 Thaliana. *Plant Cell* 2(3):235-243.
486 13. Masucci JD & Schiefelbein JW (1994) The Rhd6 Mutation of Arabidopsis-Thaliana Alters Root-Hair
487 Initiation through an Auxin-Associated and Ethylene-Associated Process. *Plant Physiol*
488 106(4):1335-1346.
489 14. Masucci JD & Schiefelbein JW (1996) Hormones act downstream of TTG and GL2 to promote root
490 hair outgrowth during epidermis development in the Arabidopsis root. *Plant Cell* 8(9):1505-1517.
491 15. Rerie WG, Feldmann KA, & Marks MD (1994) The Glabra2 Gene Encodes a Homeo Domain Protein
492 Required for Normal Trichome Development in Arabidopsis. *Gene Dev* 8(12):1388-1399.
493 16. Lee MM & Schiefelbein J (1999) WEREWOLF, a MYB-related protein in arabidopsis, is a position-
494 dependent regulator of epidermal cell patterning. *Cell* 99(5):473-483.
495 17. Galway ME*, et al.* (1994) The Ttg Gene Is Required to Specify Epidermal-Cell Fate and Cell
496 Patterning in the Arabidopsis Root. *Dev Biol* 166(2):740-754.
497 18. Di Cristina M*, et al.* (1996) The Arabidopsis Athb-10 (GLABRA2) is an HD-Zip protein required for
498 regulation of root hair development. *Plant J* 10(3):393-402.
499 19. Shibata M & Sugimoto K (2019) A gene regulatory network for root hair development. *J Plant Res*
500 132(3):301-309.
501 20. Grebe M (2012) The patterning of epidermal hairs in Arabidopsis - updated. *Curr Opin Plant Biol*
502 15(1):31-37.
503 21. Schiefelbein J, Huang L, & Zheng XH (2014) Regulation of epidermal cell fate in Arabidopsis roots:
504 the importance of multiple feedback loops. *Front Plant Sci* 5.
505 22. Chapman JM, Muhlemann JK, Gayornba SR, & Muday GK (2019) RBOH-Dependent ROS Synthesis
506 and ROS Scavenging by Plant Specialized Metabolites To Modulate Plant Development and Stress
507 Responses. *Chem Res Toxicol* 32(3):370-396.

508 23. Bienert GP*, et al.* (2007) Specific aquaporins facilitate the diffusion of hydrogen peroxide across
509 membranes. *J Biol Chem* 282(2):1183-1192.
510 24. Poole LB & Schoneich C (2015) Introduction: What we do and do not know regarding redox
511 processes of thiols in signaling pathways. *Free Radical Bio Med* 80:145-147.
512 25. Suzuki N*, et al.* (2011) Respiratory burst oxidases: the engines of ROS signaling. *Curr Opin Plant*
513 *Biol* 14(6):691-699.
514 26. Kobayashi M*, et al.* (2007) Calcium-dependent protein kinases regulate the production of reactive
515 oxygen species by potato NADPH oxidase. *Plant Cell* 19(3):1065-1080.
516 27. Postiglione AE & Muday GK (2020) The Role of ROS Homeostasis in ABA-Induced Guard Cell
517 Signaling. *Front Plant Sci* 11.
518 28. Mittler R*, et al.* (2011) ROS signaling: the new wave? *Trends Plant Sci* 16(6):300-309.
519 29. Kwak JM*, et al.* (2003) NADPH oxidase AtrbohD and AtrbohF genes function in ROS-dependent
520 ABA signaling in Arabidopsis. *Embo J* 22(11):2623-2633.
521 30. Mangano S*, et al.* (2017) Molecular link between auxin and ROS-mediated polar growth. *P Natl*
522 *Acad Sci USA* 114(20):5289-5294.
523 31. Tanimoto M, Roberts K, & Dolan L (1995) Ethylene is a positive regulator of root hair development
524 in Arabidopsis thaliana. *Plant J* 8(6):943-948.
525 32. Bleecker AB (1999) Ethylene perception and signaling: an evolutionary perspective. *Trends Plant*
526 *Sci* 4(7):269-274.
527 33. Binder BM (2020) Ethylene signaling in plants. *J Biol Chem* 295(22):7710-7725.
528 34. Kieber JJ, Rothenberg M, Roman G, Feldmann KA, & Ecker JR (1993) Ctr1, a Negative Regulator of
529 the Ethylene Response Pathway in Arabidopsis, Encodes a Member of the Raf Family of Protein-
530 Kinases. *Cell* 72(3):427-441.
531 35. Alonso JM, Hirayama T, Roman G, Nourizadeh S, & Ecker JR (1999) EIN2, a bifunctional transducer
532 of ethylene and stress responses in Arabidopsis. *Science* 284(5423):2148-2152.
533 36. Ju CL*, et al.* (2012) CTR1 phosphorylates the central regulator EIN2 to control ethylene hormone
534 signaling from the ER membrane to the nucleus in Arabidopsis. *P Natl Acad Sci USA*
535 109(47):19486-19491.
536 37. Wen X*, et al.* (2012) Activation of ethylene signaling is mediated by nuclear translocation of the
537 cleaved EIN2 carboxyl terminus. *Cell Res* 22(11):1613-1616.
538 38. Feng Y*, et al.* (2017) Ethylene promotes root hair growth through coordinated EIN3/EIL1 and
539 RHD6/RSL1 activity in Arabidopsis. *P Natl Acad Sci USA* 114(52):13834-13839.
540 39. Harkey AF*, et al.* (2018) Identification of Transcriptional and Receptor Networks That Control Root
541 Responses to Ethylene. *Plant Physiol* 176(3):2095-2118.
542 40. Lim SD, Kim SH, Gilroy S, Cushman JC, & Choi WG (2019) Quantitative ROS bioreporters: A robust
543 toolkit for studying biological roles of ROS in response to abiotic and biotic stresses. *Physiol*
544 *Plantarum* 165(2):356-368.
545 41. Dickinson BC, Huynh C, & Chang CJ (2010) A Palette of Fluorescent Probes with Varying Emission
546 Colors for Imaging Hydrogen Peroxide Signaling in Living Cells. *J Am Chem Soc* 132(16):5906-5915.
547 42. Hua J & Meyerowitz EM (1998) Ethylene responses are negatively regulated by a receptor gene
548 family in Arabidopsis thaliana. *Cell* 94(2):261-271.
549 43. Solano R, Stepanova A, Chao QM, & Ecker JR (1998) Nuclear events in ethylene signaling: a
550 transcriptional cascade mediated by ETHYLENE-INSENSITIVE3 and ETHYLENE-RESPONSE-
551 FACTOR1. *Gene Dev* 12(23):3703-3714.
552 44. Chao QM*, et al.* (1997) Activation of the ethylene gas response pathway in Arabidopsis by the
553 nuclear protein ETHYLENE-INSENSITIVE3 and related proteins. *Cell* 89(7):1133-1144.

554 45. Harkey AF, Yoon GM, Seo DH, DeLong A, & Muday GK (2019) Light Modulates Ethylene Synthesis,
555 Signaling, and Downstream Transcriptional Networks to Control Plant Development. *Front Plant*
556 *Sci* 10.
557 46. Guzman P & Ecker JR (1990) Exploiting the Triple Response of Arabidopsis to Identify Ethylene-
558 Related Mutants. *Plant Cell* 2(6):513-523.
559 47. Jones MA, Raymond MJ, Yang ZB, & Smirnoff N (2007) NADPH oxidase-dependent reactive oxygen
560 species formation required for root hair growth depends on ROP GTPase. *J Exp Bot* 58(6):1261-
561 1270.
562 48. Takeda S*, et al.* (2008) Local positive feedback regulation determines cell shape in root hair cells.
563 *Science* 319(5867):1241-1244.
564 49. Negi S, Sukumar P, Liu X, Cohen JD, & Muday GK (2010) Genetic dissection of the role of ethylene
565 in regulating auxin-dependent lateral and adventitious root formation in tomato. *Plant J* 61(1):3-
566 15.
567 50. Lewis DR, Negi S, Sukumar P, & Muday GK (2011) Ethylene inhibits lateral root development,
568 increases IAA transport and expression of PIN3 and PIN7 auxin efflux carriers. *Development*
569 138(16):3485-3495.
570 51. Shigeto J & Tsutsumi Y (2016) Diverse functions and reactions of class III peroxidases. *New Phytol*
571 209(4):1395-1402.
572 52. Liszkay A, Kenk B, & Schopfer P (2003) Evidence for the involvement of cell wall peroxidase in the
573 generation of hydroxyl radicals mediating extension growth. *Planta* 217(4):658-667.
574 53. Passardi F, Cosio C, Penel C, & Dunand C (2005) Peroxidases have more functions than a Swiss
575 army knife. *Plant Cell Rep* 24(5):255-265.
576 54. Datta S, Prescott H, & Dolan L (2015) Intensity of a pulse of RSL4 transcription factor synthesis
577 determines Arabidopsis root hair cell size. *Nat Plants* 1(10).
578 55. Binder BM*, et al.* (2007) The Arabidopsis EIN3 binding F-box proteins EBF1 and EBF2 have distinct
579 but overlapping roles in ethylene signaling. *Plant Cell* 19(2):509-523.
580 56. Marzol E, Borassi, C., Ranocha, P., Aptekman, A.A., Bringas, M., Pennington, J., Paez-Valencia, J.,
581 Pacheco, J.M., Garcia, D.R.R., Guerrero, Y.D.C, Carignani, M., Mangano, S., Fleming, M., Mishler-
582 Elmore, J.W., Blanco-Herrera, F., Bedinger, P., Dunand, C., Capece, L., Nadra, A.D., Held, M.,
583 Otegu, M., Estevez, J.M (2021) Class III peroxidases PRX01, PRX44, and PRX73 potentially target
584 extensins during root hair growth in Arabidopsis thaliana.
585 57. Chu-Puga A, Gonzalez-Gordo S, Rodriguez-Ruiz M, Palma JM, & Corpas FJ (2019) NADPH Oxidase
586 (Rboh) Activity is Up Regulated during Sweet Pepper (Capsicum annuum L.) Fruit Ripening.
587 *Antioxidants-Basel* 8(1).

588

589

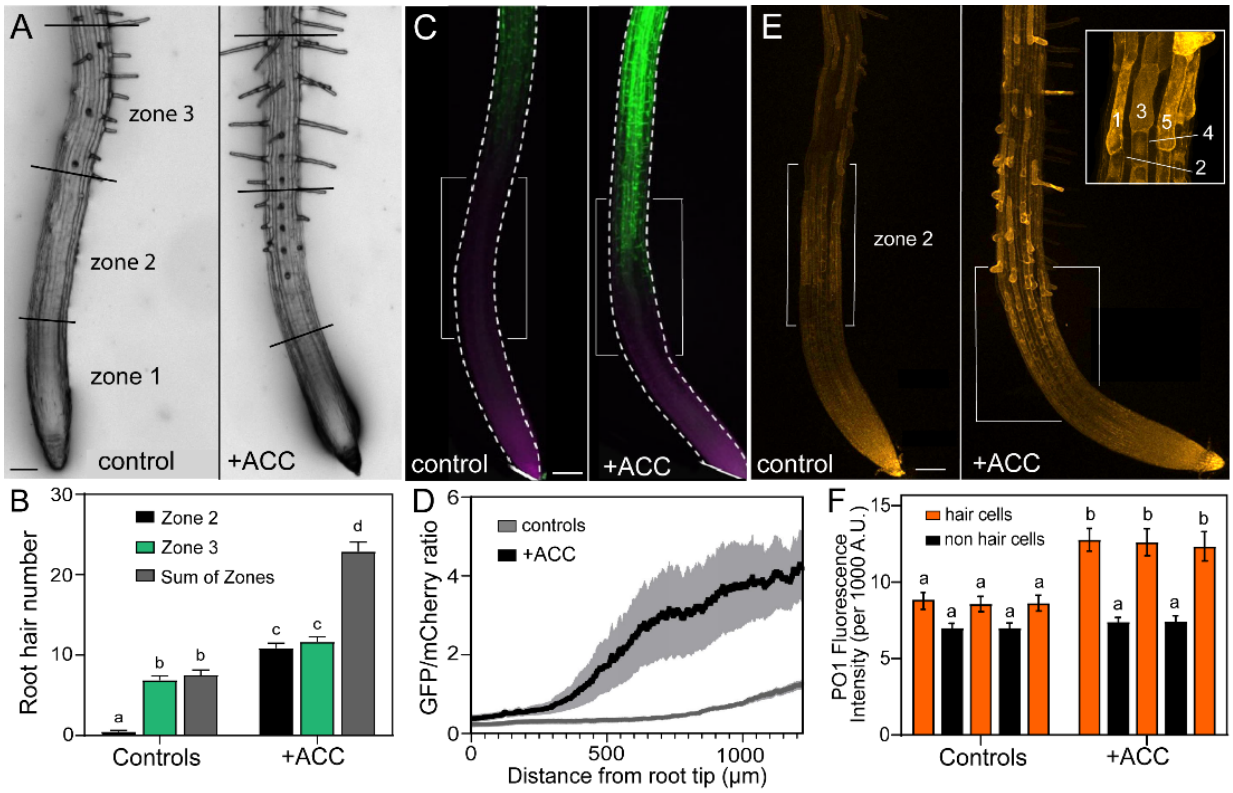


**Figure 1. ACC treatment induced root hair number, ROS dependent gene expression along the root, and $H_2O_2$ accumulation in trichoblasts after 4 hours** (A) Representative images of root tips in Col-0 treated with and without ACC for 4 hours. Zones 1, 2, and 3 represent 500 µm root sections. Scale bar for all images are 100 µm. (B) Root hair quantification of untreated and 4h ACC treated seedlings. No root hairs formed in zone 1. Data are means ± SEM of total RH in zone 2, zone 3, and all zones from 3 experiments (n=18-24 seedlings per experiment). Columns with different letters indicate statistically significant differences determined by two-way ANOVA followed by Tukey's multiple comparisons test. (C) Representative images of root tips of Col-0 containing the ZAT12p-ROS reporter treated with or without ACC for 4 hours with GFP signal in green and mCherry signal in magenta. White brackets indicate zone 2 of the root. (D) Quantification of the ratio of GFP/mCherry fluorescence intensity using a line profile along the roots of an average of 6-12 seedlings of 3 independent experiments of untreated or ACC treated seedlings. Data are means ± SEM (E) Representative roots illustrating the alternating PO1 fluorescence between trichoblast and atrichoblast epidermal cell files of cells in Col-0 roots with and without ACC treatment for 4 hours. White brackets indicate zone 2 of the root. Inset indicates hair cells (1, 3, 5) vs. non hair cells (2, 4). (F) Quantification of PO1 fluorescence intensity in trichoblasts (orange bars: 1, 3 and 5) and atrichoblasts (black bars: 2, 4). Data are means ± SEM of 3 independent experiments (n=18-24 seedlings/experiment). The error is too small to see in untreated roots. Columns with different letters indicate statistical significance compared to Col-0 untreated cells as determined by two-way ANOVA followed by Tukey's multiple comparisons test.

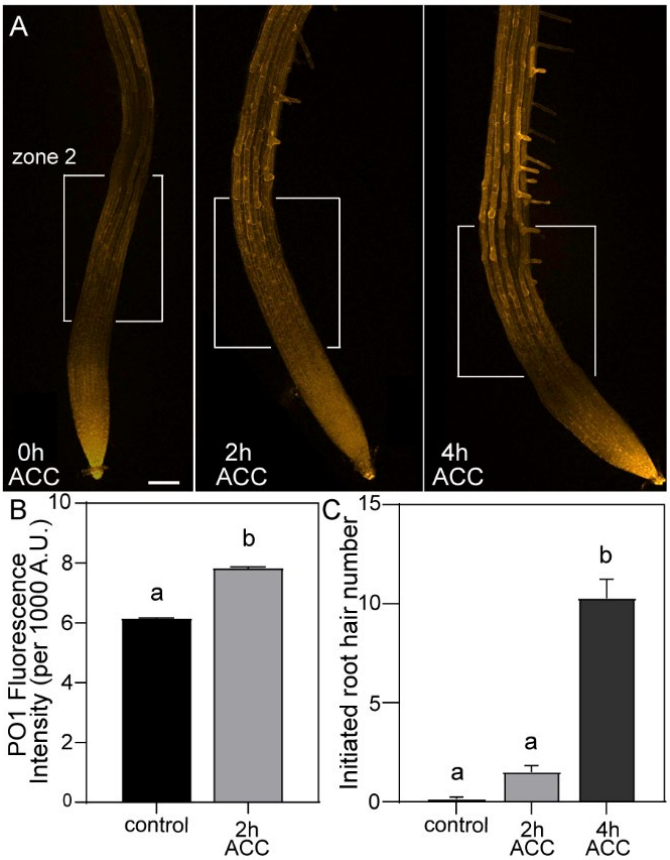


**Figure 2. Ethylene-induced ROS accumulation preceded root hair initiation.** (A) Representative images of epidermal PO1 fluorescence in untreated Col-0 and Col-0 treated with ACC for 2 or 4h. Scale bar is 100 µm. White brackets indicate zone 2 of the root. (B) Quantification of trichoblasts that had not yet formed root hair bulges of control and 2h ACC treated seedlings. (C) Quantification of number of initiated root hairs in zone 2 of the root (500 µm-1000 µm from root tip) in untreated and 2 and 4h ACC-treated seedlings. Data are mean ± SEM of individual cells from 3 independent experiments (n= 12-18 seedlings/experiment). Columns with different letters indicate statistical significance compared to untreated hair cells as determined by Student's t-test ($p < 0.0001$) in B. Columns with different letters indicate statistically significant differences determined by one-way ANOVA followed by Tukey's multiple comparisons test in C.

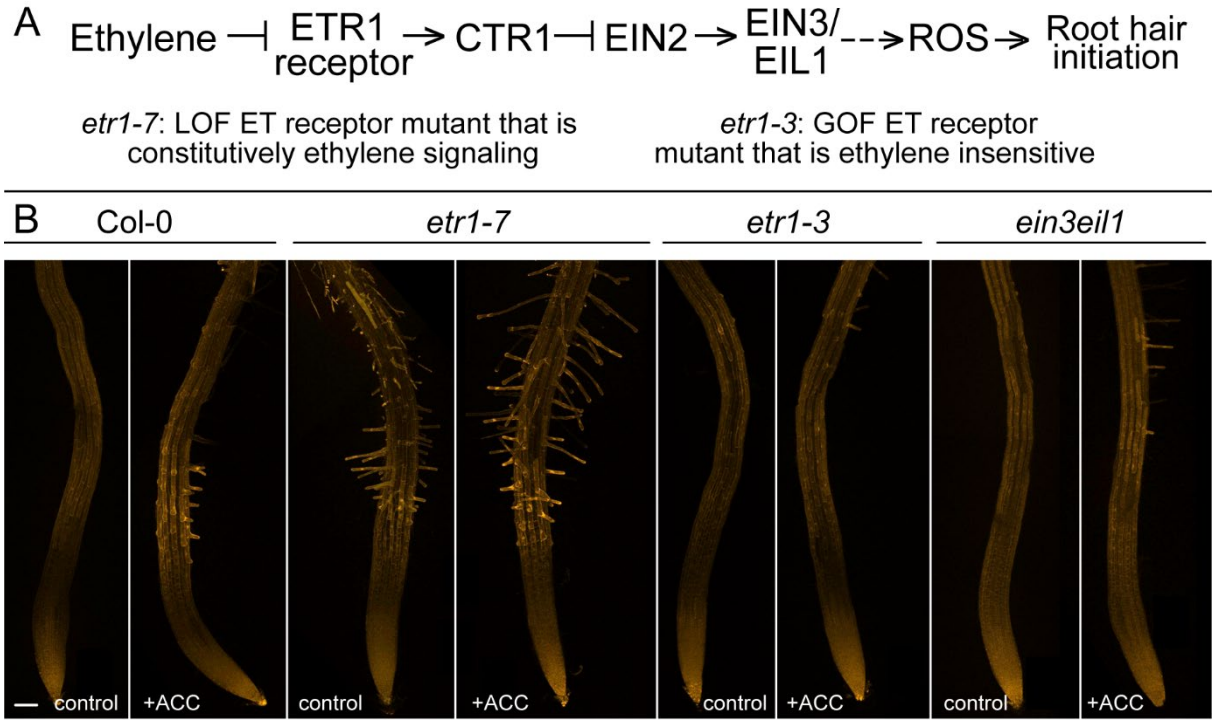


**Figure 3. The ETR1 receptor and EIN3/EIL1 transcription factors are required for ethylene-induced ROS accumulation and root hair proliferation.** (A) A schematic diagram of the ethylene signaling pathway and explanation of the character of the *etr* mutants. ETR1 (ethylene resistant 1) is the ethylene receptor controlling root hair formation, CTR1 (constitutive triple response 1 is a kinase, EIN2 (ethylene insensitive 2) is a signaling protein, EIN3 and EIL1 (EIN3-like 1) are transcription factors. (B) Representative images of PO1 epidermal fluorescence in Col-0, *etr1-7*, *etr1-3*, and *ein3-1eil1-1* treated with and without ACC for 4 hours. 18-20 seedlings from each genotype and treatment were imaged. Scale bar is 100 µm.

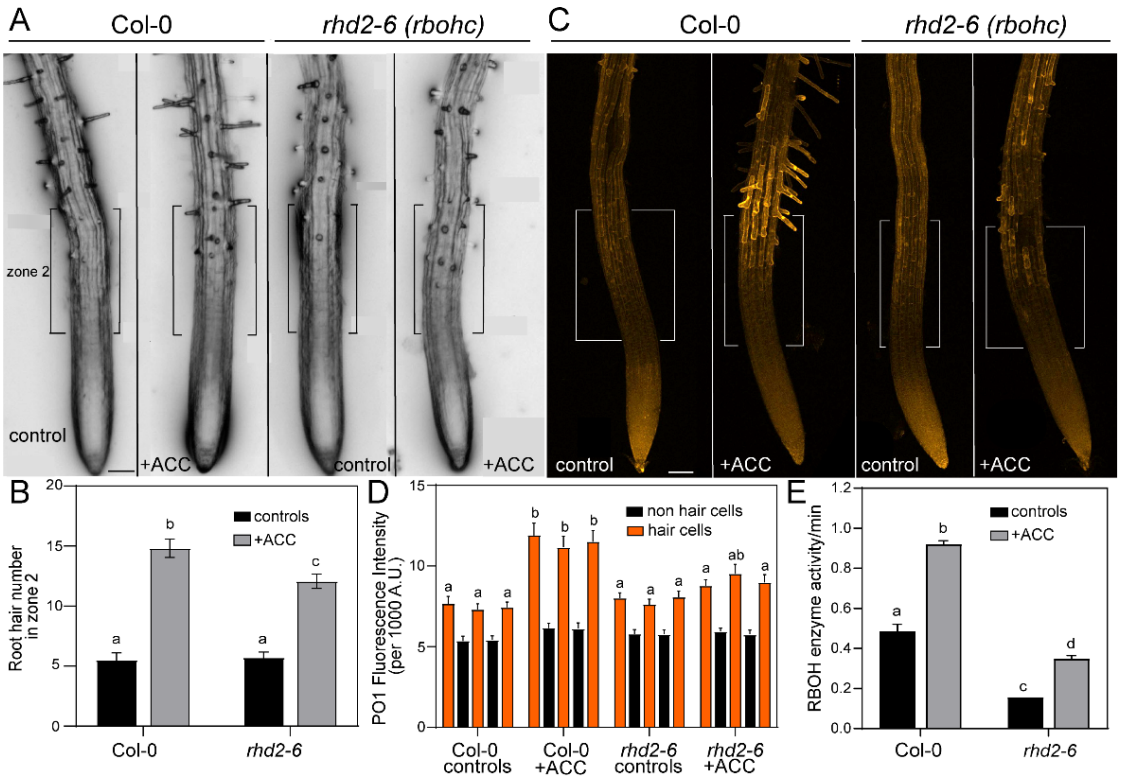


**Figure 4. RBOHC activity contributes to ethylene-induced ROS accumulation.** (A) Representative images of root hairs of Col-0 and *rhd2-6* treated with and without ACC for 4 hours. Black brackets indicate zone 2 of the root. (B) Root hair quantification of untreated and 4h ACC treated seedlings. Data are means ± SEM of total RH in zone 2 from 3 experiments (n=18-24 seedlings per experiment). Columns with different letters indicate statistically significant differences determined by two-way ANOVA followed by Tukey's multiple comparisons test. (C) Representative images of PO1 epidermal fluorescence in Col-0 and *rhd2-6* treated with and without ACC for 4 hours. White brackets indicate zone 2 of the root. (D) Quantification of PO1 fluorescence intensity in hair cells and non-hair cells. Data are means ± SEM of 3 experiments (n=18-24 seedlings/experiment). Columns with different letters indicate statistical significance in PO1 signal compared to other hair cells as determined by two-way ANOVA followed by Tukey's multiple comparisons test. (E) Quantification of formazan concentration per minute in roots of Col-0 and *rhd2-6* treated with and without ACC for 4 hours. Data are means ± SEM of 3 experiments. Columns with different letters indicate statistical significance as determined by two-way ANOVA followed by Tukey's multiple comparisons test. Scale bars for all images are 100 µm.

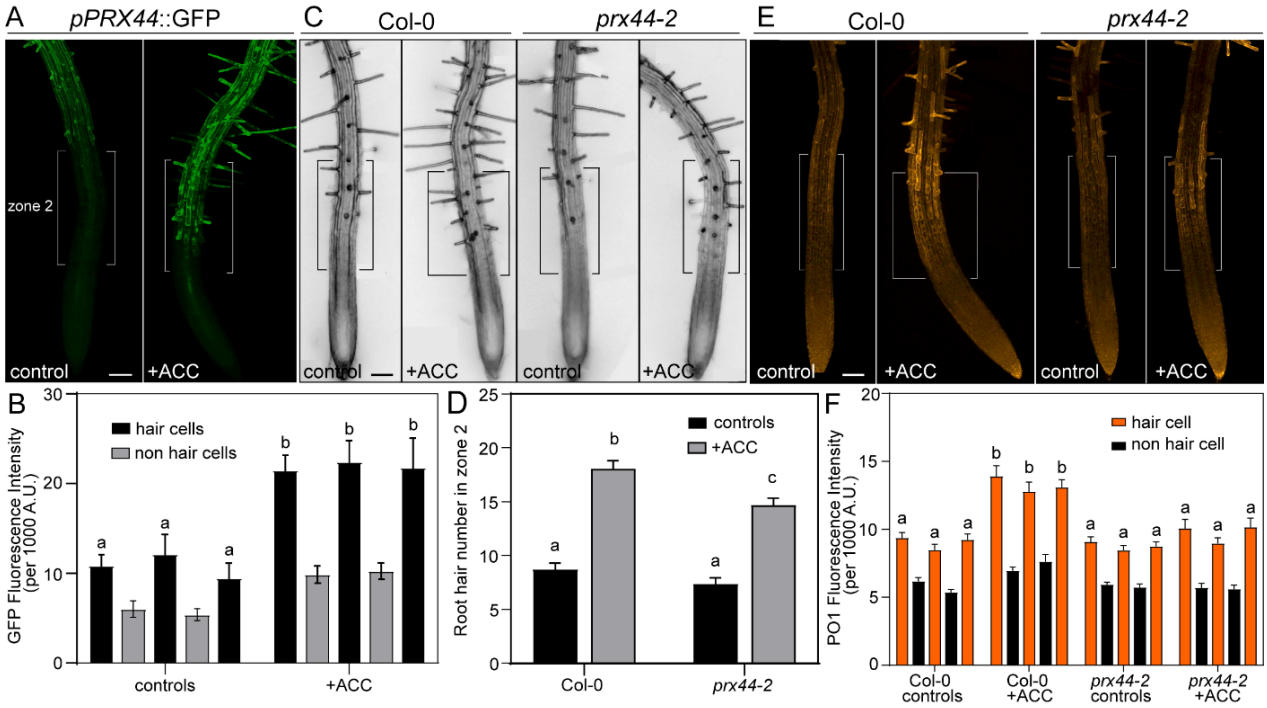


**Figure 5. *pPRX44*::GFP expression increases in roots treated with ACC and PRX44 contributes to ethylene-induced root hair formation and $H_2O_2$ accumulation in root hair cells** (A) Representative images of *pPRX44*::GFP treated with and without ACC for 4 hours. White brackets indicate zone 2 of the root. (B) Quantification of GFP signal in hair and non-hair cells of *pPRX44*::GFP treated with and without ACC. Data are means ± SEM (C) Representative images of RH number in Col-0 and *prx44-2* treated with and without ACC for 4 hours. Black brackets indicate zone 2 of the root. (D) Root hair quantification of untreated and 4h ACC treated seedlings. Data are means ± SEM. of 3 independent experiments (n=18-24 seedlings per experiment). Columns with different letters indicated statistically significant differences determined by two-way ANOVA followed by Tukey's multiple comparison test. (E) Representative images of Col-0 and *prx44-2* treated with and without ACC for 4 hours and stained with PO1. White brackets indicate zone 2 of the root. (F) Quantification of PO1 accumulation in hair and non-hair cells of Col-0 and *prx44-2* treated with and without ACC for 4 hours (n=12-18 seedlings per experiment). Data are means ± SEM of 3 experiments. Columns with different letters indicate statistical significance compared to all other hair cells as determined by two-way ANOVA followed by Tukey's multiple comparisons test. Scale bars for all images are 100 µm.

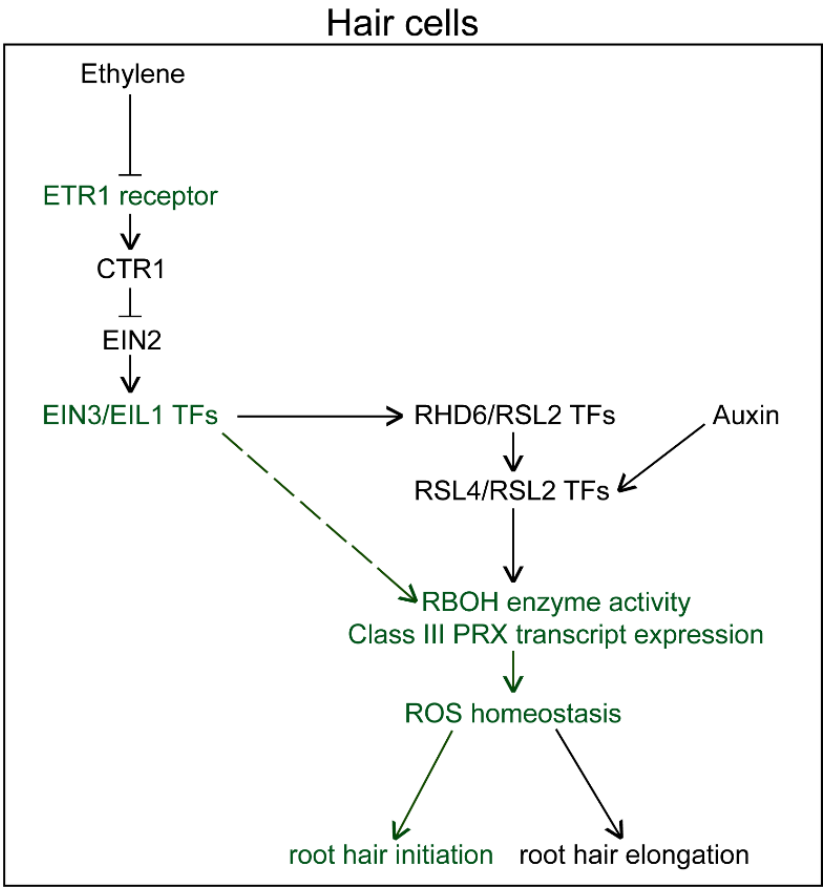


**Figure 6. Summary of mechanisms by which ethylene and auxin modulate ROS and root hair formation**. In hair cells, ethylene, acting through the ETR1 receptor and the canonical ethylene signaling pathway induces accumulation of EIN3/EIL1 TF proteins. Previous work has shown that EIN3/EIL1 physically interacts with RHD6/RSL2 TFs to induce expression of RSL4/RSL2 transcripts leading to root hair elongation (38). It has also been shown that RSL4/RSL2 is induced by auxin signaling and that RSL4/RSL2 binds to the promoters of RBOH and class III PRX genes to induce transcript expression and root hair elongation (30). Here, highlighted in green, we have shown that ethylene signaling through ETR1 and EIN3/EIL1 induces ROS accumulation through RBOHC enzyme activity and PRX44 transcript expression to drive root hair initiation.